Sensor shape design for piezoelectric cantilever beams to harvest vibration energy

Michael I. Friswell[a] and Sondipon Adhikari
School of Engineering, Swansea University, Singleton Park, Swansea SA2 8PP, United Kingdom

(Received 13 May 2010; accepted 29 May 2010; published online 6 July 2010)

Energy harvesting for the purpose of powering low power electronic sensor systems has received explosive attention in the last few years. A common device uses the piezoelectric effect for a cantilever beams at resonance to harvest ambient vibration energy. However most of these devices have a rectangular piezoelectric patch covering all or part of the beam. This paper considers the optimum design of such a device, and in particular investigates the effect that the size and shape of piezoelectric sensor has on the harvested energy. It is shown that significant increases in harvested energy may be obtained by optimising the sensor design. © *2010 American Institute of Physics*. [doi:10.1063/1.3457330]

I. INTRODUCTION

The harvesting of ambient vibration energy for use in powering low energy electronic devices has formed the focus of much recent research.[1–4] Energy harvesting of ambient vibration has become important and new electronic devices are being developed that require very low power. Completely wireless sensor systems are desirable and this can only be accomplished by using batteries and/or harvested energy. Harvesting is attractive because harvested energy can be used directly or used to recharge batteries or other storage devices, which enhances battery life. Of the published results that focus on the piezoelectric effect as the transduction method, only a small part is concerned with random excitation[5,6] and almost all has focused on harvesting using cantilever beams and on single frequency ambient energy, i.e., resonance based energy harvesting. Several authors[7–11] have proposed methods to optimize the parameters of the system to maximize the harvested energy.

Erturk and Inman[12–14] developed the equations of motion for cantilever beam energy harvesters. Goldschmidtboeing and Woias[15] and Dietl and Garcia[16] considered the effect of different beam shapes on the harvested energy. Schoeftner and Irschik[17] considered shaped transducers for increasing passive damping, which is closely related to energy harvesting. Kaal *et al.*[18] considered energy harvesters with piezoelectric transducers that only covered part of the beam. Rupp *et al.*[19] used topology optimization to design the shape of the piezoelectric layers in harvesters constructed of plates and shells.

This paper considers beam energy harvesters clamped at one end to a support that vibrates sinusoidally. The novel feature of this analysis is the incorporation of a piezoelectric transducer whose width can be varied along the beam length. Shaped piezoelectric sensors are well established for modal control[20] and applications are emerging in structural health monitoring.[21] The approach specifies the shape of the sensor by the width and the slope at the finite element nodes; this allows the shape to be specified easily using a small number of variables, and makes the optimization of the shape possible.

II. ELECTROMECHANICAL MODEL OF A CANTILEVER BEAM HARVESTER

The energy harvester consists of a cantilever beam whose support is subjected to motion from the host structure. The development in this paper will assume that the motion of the beam support may be translational and rotational. The system is shown schematically in Fig. 1, although only the translational support motion, $u(t)$, is shown. The beam is not necessarily uniform, and discrete masses may be added to the beam. The mechanical parts of this model, and the excitation from the support motion, are standard.

We now concentrate on the electromechanical coupling. Suppose that the displacement of the beam is given by $w(x)$, where x is the position along the beam. This displacement is the elastic deformation, that is the displacement relative to the rigid body displacement due to the support excitation. The constant thickness piezoelectric material is placed along the beam, and the effective width is given by $f(x)$. The variable width would most likely be implemented by varying the width of the electrode while keeping the width of piezoelectric material constant. The current output is then given by

$$i_p = -e_{31}h\int_0^L f(x)\frac{\partial^3 w}{\partial x^2\,\partial t}\mathrm{d}x, \tag{1}$$

where h is the distance of the piezoelectric material from the beam centerline (assuming the beam is uniform and the piezoelectric layer is very thin) and e_{31} is the piezoelectric constant. This equation assumes that the material is operating

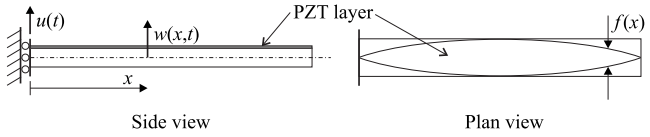

FIG. 1. Schematic of the cantilever beam energy harvester excited at the support.

[a]Electronic mail: m.i.friswell@swansea.ac.uk.

in the 31 mode, which is the case for a thin layer of homogeneous piezoelectric material on the beam with the electrodes on the top and bottom surfaces; a similar equation may be developed for transducers with interdigitated electrodes.

If the system is modeled with finite element analysis, using standard Euler–Bernoulli beam elements, then we may derive the free-free mass and stiffness matrices $\mathbf{M}_{ff}$ and $\mathbf{K}_{ff}$. Assuming that the beam is clamped at one end and this support motion has translational and rotational motion given by $u(t)$ and $\psi(t)$, respectively, then the kinetic and potential energies of the beam, T and U, are

$$T = \begin{Bmatrix} \dot{u} \\ \dot{\psi} \\ \dot{q}_1 + \dot{u} + x_2\dot{\psi} \\ \dot{q}_2 + \dot{\psi} \\ \dot{q}_3 + \dot{u} + x_3\dot{\psi} \\ \vdots \end{Bmatrix}^{\top} \mathbf{M}_{ff} \begin{Bmatrix} \dot{u} \\ \dot{\psi} \\ \dot{q}_1 + \dot{u} + x_2\dot{\psi} \\ \dot{q}_2 + \dot{\psi} \\ \dot{q}_3 + \dot{u} + x_3\dot{\psi} \\ \vdots \end{Bmatrix}$$

$$= \dot{\mathbf{q}}^{\top}\mathbf{M}\dot{\mathbf{q}} + 2\dot{\mathbf{q}}^{\top}\mathbf{B}_M \begin{Bmatrix} \dot{u} \\ \dot{\psi} \end{Bmatrix} + \begin{Bmatrix} \dot{u} \\ \dot{\psi} \end{Bmatrix}^{\top} \mathbf{E}_M \begin{Bmatrix} \dot{u} \\ \dot{\psi} \end{Bmatrix} \tag{2}$$

and

$$U = \begin{Bmatrix} 0 \\ 0 \\ \mathbf{q} \end{Bmatrix}^{\top} \mathbf{K}_{ff} \begin{Bmatrix} 0 \\ 0 \\ \mathbf{q} \end{Bmatrix} = \mathbf{q}^{\top}\mathbf{K}\mathbf{q}, \tag{3}$$

where $\mathbf{q}=[q_1 q_2 \ldots]^{\top}$ are the nodal generalized displacements of the beam model, not including the node at the support, and are defined relative to the rigid body motion of the beam. The dot denotes the derivative with respect to time and x_i is the distance of the ith node from the support. $\mathbf{M}$ and $\mathbf{K}$ are the standard mass and stiffness matrices for the beam with cantilever boundary conditions. The matrix $\mathbf{B}_M$ is obtained from the columns of the free-free mass matrix, and is given by

$$\mathbf{B}_M = [0 \quad \mathbf{I}]\mathbf{M}_{ff} \begin{bmatrix} 1 & 0 \\ 0 & 1 \\ 1 & x_2 \\ 0 & 1 \\ 1 & x_3 \\ \vdots & \vdots \end{bmatrix}, \tag{4}$$

where 0 is the $n \times 2$ zero matrix and $\mathbf{I}$ is the $n \times n$ identity matrix, where n is the number of degrees of freedom (length of the vector $\mathbf{q}$).

We then obtain the equations of motion as

$$\mathbf{M}\ddot{\mathbf{q}} + \mathbf{D}\dot{\mathbf{q}} + \mathbf{K}\mathbf{q} = \mathbf{Q}_p - \mathbf{B}_M \begin{Bmatrix} \ddot{u} \\ \ddot{\psi} \end{Bmatrix}, \tag{5}$$

where $\mathbf{Q}_p$ is the force arising from charge on the piezoelectric material. Note that a damping matrix, $\mathbf{D}$, has been included which represents internal damping in the beam; if other damping mechanisms were included, for example, air damping, then a term dependent on the support generalized velocities would also appear on the right side of the equations of motion.

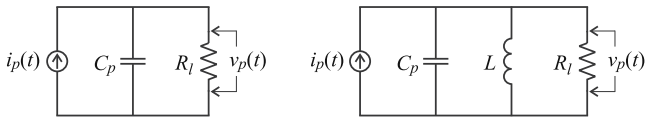

(a) without inductor (b) with inductor

FIG. 2. The two electrical circuits for the harvester (a) without an inductor, (b) with an inductor.

Using the finite element displacement functions, the charge on the piezoelectric material may be estimated for each element and the total charge obtained by summing the charge over the elements. This is exactly the same as the development for shaped sensors for control or structural health monitoring.[20,21] For a beam element with cubic shape functions,[20] the current generated by the piezoelectric is the time derivative of the charge produced, and is

$$i_{pe}(t) = -\mathbf{f}_e^{\top}\mathbf{C}_{pe}\dot{\mathbf{q}}_e, \tag{6}$$

where

$$\mathbf{C}_{pe} = \frac{e_{31}h}{30\ell_e} \begin{bmatrix} 36 & 33\ell_e & -36 & 3\ell_e \\ 3\ell_e & 4\ell_e^2 & -3\ell_e & -\ell_e^2 \\ -36 & -3\ell_e & 36 & -33\ell_e \\ 3\ell_e & -\ell_e^2 & -3\ell_e & 4\ell_e^2 \end{bmatrix}, \tag{7}$$

ℓ_e is the element length, $\mathbf{q}_e$ are generalized displacements for the element, and $\mathbf{f}_e$ is the piezoelectric shape defined at the element nodes. Adding the contributions for all nodes gives the total current produced as

$$i_p = -\mathbf{f}^{\top}\mathbf{C}_{pq}\dot{\mathbf{q}} - \mathbf{f}^{\top}\mathbf{C}_{ps} \begin{Bmatrix} \dot{u} \\ \dot{\psi} \end{Bmatrix}, \tag{8}$$

where $\mathbf{C}_{pq}$ and $\mathbf{C}_{ps}$ are matrices that are easily assembled from element coupling matrices, Eq. (7), and $\mathbf{f}$ is a vector that defines the sensor shape.[20,21] The last term in Eq. (8) arises because of the imposed motion at the beam support. $\mathbf{f}$ actually gives the transducer width and slope at the nodes of the finite element model, and the shape within the elements is approximated using the beam shape functions.

The force on the beam from the piezoelectric material is given by

$$\mathbf{Q}_p = \mathbf{C}_{pq}^{\top}\mathbf{f}v_p, \tag{9}$$

where $v_p(t)$ is the voltage across the piezoceramic. Thus

$$\mathbf{M}\ddot{\mathbf{q}} + \mathbf{D}\dot{\mathbf{q}} + \mathbf{K}\mathbf{q} - \mathbf{C}_{pq}^{\top}\mathbf{f}v_p = -\mathbf{B}_M \begin{Bmatrix} \ddot{u} \\ \ddot{\psi} \end{Bmatrix}. \tag{10}$$

III. SIMPLE ELECTRICAL CIRCUITS FOR THE ENERGY HARVESTER

Figure 2 shows two simple electrical circuits that will be modeled to investigate the performance of the energy harvester. The governing equations are obtained using Kir-

choff's laws, where the current generated in the piezoelectric material is given by Eq. (8). Thus, without the inductor [case (a)], the governing electrical equation is

$$\mathbf{f}^{\top}\mathbf{C}_{pq}\dot{\mathbf{q}} + \mathbf{f}^{\top}\mathbf{C}_{ps}\begin{Bmatrix}\dot{u}\\ \dot{\psi}\end{Bmatrix} + C_p\dot{v}_p + \frac{1}{R_l}v_p = 0, \tag{11}$$

where the load resistance is R_l, and the capacitance of the piezoceramic is C_p.

When an inductor is included [case (b)] the governing equation is

$$\mathbf{f}^{\top}\mathbf{C}_{pq}\ddot{\mathbf{q}} + \mathbf{f}^{\top}\mathbf{C}_{ps}\begin{Bmatrix}\ddot{u}\\ \ddot{\psi}\end{Bmatrix} + C_p\ddot{v}_p + \frac{1}{R_l}\dot{v}_p + \frac{1}{L}v_p = 0, \tag{12}$$

where L is the inductance of the circuit.

One important feature of the shaped transducer is that the capacitance of the piezoelectric device depends on the area of the electrode, and therefore the shape of the electrode. Thus

$$C_p = \frac{\epsilon_{33}}{t_p}\int_0^L |f(x)|\mathrm{d}x, \tag{13}$$

where ϵ_{33} is a constant, t_p is the thickness of the piezoelectric material. If the sensor width is always positive or always negative then it is possible to perform the integration using the beam element shape functions to obtain

$$C_p = \mathbf{f}^{\top}\mathbf{g}, \tag{14}$$

where $\mathbf{g}$ is a vector calculated from the shape functions. However if the sensor width changes sign, which usually occurs within an element, then there is no closed form expression for the capacitance in terms of the nodal values defining the sensor. Thus in the general case Eq. (13) has to be calculated numerically. Note that the change in sign for the sensor width denotes a change in polarity in the electrical connections to the piezoceramic.

IV. SINGLE MODE ELECTROMECHANICAL MODEL FOR RESONANT HARVESTER

Often the energy harvester is designed to be resonant, as this increases the power output of the harvester for a fixed frequency excitation. Thus one of the natural frequencies of the harvester corresponds to the excitation frequency, and the deformation shape of the beam is dominated by a single mode. Suppose the rth mode is excited, then we may approximate the response using a single degree of freedom, namely the rth principal coordinate p_r, so that

$$\mathbf{q} = \boldsymbol{\phi}_r p_r, \tag{15}$$

where $\boldsymbol{\phi}_r$ is the rth mode shape. Substituting this displacement into Eq. (5), using Eq. (9) and premultiplying by $\boldsymbol{\phi}_r^{\top}$, gives the single degree of freedom mechanical model as

$$\ddot{p}_r + 2\zeta_r\omega_r\dot{p}_r + \omega_r^2 p_r - \frac{\theta_r}{m_r}v_p = \mathbf{B}_{Mr}\begin{Bmatrix}\ddot{u}\\ \ddot{\psi}\end{Bmatrix}, \tag{16}$$

where ζ_r and ω_r are the rth damping ratio and natural frequency, $m_r = \boldsymbol{\phi}_r^{\top}\mathbf{M}\boldsymbol{\phi}_r$ is the rth modal mass, and

$$\theta_r = \boldsymbol{\phi}_r^{\top}\mathbf{C}_{pq}^{\top}\mathbf{f}. \tag{17}$$

The base excitation coefficient matrix is

$$\mathbf{B}_{Mr} = \boldsymbol{\phi}_r^{\top}\mathbf{B}_M/m_r. \tag{18}$$

The equations governing the electrical circuit become,

$$\theta_r\dot{p}_r + C_p\dot{v}_p + \frac{1}{R_l}v_p = -\mathbf{f}^{\top}\mathbf{C}_{ps}\begin{Bmatrix}\dot{u}\\ \dot{\psi}\end{Bmatrix}, \tag{19}$$

without the inductor, or

$$\theta_r\ddot{p}_r + C_p\ddot{v}_p + \frac{1}{R_l}\dot{v}_p + \frac{1}{L}v_p = -\mathbf{f}^{\top}\mathbf{C}_{ps}\begin{Bmatrix}\ddot{u}\\ \ddot{\psi}\end{Bmatrix}, \tag{20}$$

with the inductor.

A. Power generated under resonant harmonic excitation

Suppose now that the beam support is excited sinusoidally in translation only, so that

$$u(t) = u_0\cos\omega t = \Re\{u_0 e^{\mathrm{i}\omega t}\}, \quad \psi(t) = 0, \tag{21}$$

where the excitation frequency, ω, is assumed to be constant and $\mathrm{i} = \sqrt{-1}$. Then Eq. (16) becomes

$$\ddot{p}_r + 2\zeta_r\omega_r\dot{p}_r + \omega_r^2 p_r - \frac{\theta_r}{m_r}v_p = \Re\{-\omega^2 B_{Mr}u_0 e^{\mathrm{i}\omega t}\}, \tag{22}$$

where B_{Mr} is the first element of $\mathbf{B}_{Mr}$. Looking for solutions of the form,

$$p_r(t) = \Re\{P_r(\omega)e^{\mathrm{i}\omega t}\} \quad \text{and} \quad v_p(t) = \Re\{V_p(\omega)e^{\mathrm{i}\omega t}\}, \tag{23}$$

where P_r and V_p are complex, gives

$$(-\omega^2 + 2\zeta_r\omega_r\mathrm{i}\omega + \omega_r^2)P_r - \frac{\theta_r}{m_r}V_p = -\omega^2 B_{Mr}u_0. \tag{24}$$

Equation (19), for the electrical circuit without the inductor, becomes

$$\theta_r\mathrm{i}\omega P_r + \left(C_p\mathrm{i}\omega + \frac{1}{R_l}\right)V_p = -\mathbf{f}^{\top}\mathbf{C}_{psu}\mathrm{i}\omega u_0, \tag{25}$$

where $\mathbf{C}_{psu}$ is the first column of $\mathbf{C}_{ps}$.

For the case with the inductor, Eq. (25), becomes

$$-\theta_r\omega^2 P_r + \left(-C_p\omega^2 + \frac{\mathrm{i}\omega}{R_l} + \frac{1}{L}\right)V_p = \mathbf{f}^{\top}\mathbf{C}_{psu}\omega^2 u_0. \tag{26}$$

The voltage may be estimated by eliminating the displacement in Eq. (24) and one of Eqs. (25) and (26), and the amplitude of the harvested power is obtained as

$$P_{\text{out}} = \frac{|V_p|^2}{R_l}. \tag{27}$$

B. Simple approximation for the harvested power

Designing a harvester for a particular situation is difficult because all of the parameters interact. To gain some insight a number of simplifying assumptions will be made

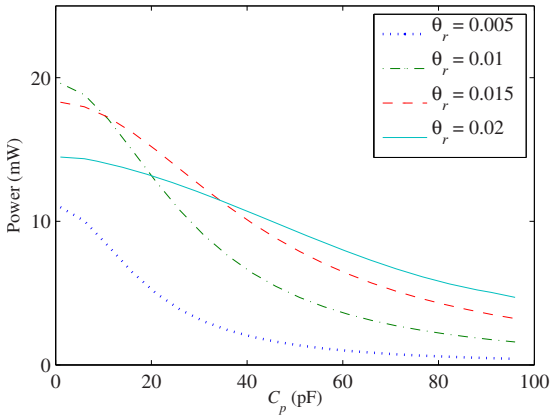

FIG. 3. (Color online) The effect of coupling coefficient and piezoelectric capacitance for the resonant harvester without an inductor.

for the system without an inductor. Suppose the load impedance is low, so that the optimum is a resonant harvester, that is $\omega=\omega_r$ for some mode (i.e., some r). Further, suppose that the resonance condition, and other constraints such as maximum harvester mass and maximum dimensions, fixes the dimensions of the beam. The excitation term on the right side of Eq. (25) will be neglected, as this will certainly be small if the lengths of the beam elements are small. The output voltage may then be written as

$$V_p = \frac{m_r\omega_r^2\theta_r B_{Mr}u_0}{c_r\left(C_p \mathrm{i}\omega_r + \frac{1}{R_l}\right) + \theta_r^2}, \tag{28}$$

where $c_r=2\zeta_r\omega_r m_r$ is the rth modal damping parameter.

Since the beam parameters are assumed to be fixed, the output voltage, and hence power harvested, for a given output load and excitation frequency, is a function of the electromechanical coupling parameter, θ_r, and the capacitance of the piezoelectric material, C_p. Both of these parameters depend on the shape of the piezoelectric transducer; as the area of coverage of the electrode increases, both C_p and θ_r tend to increase. For a typical case, where $\omega_r=100$ Hz, $R_l=100$ kΩ, $B_{Mr}=1$, $m_r=1$ kg, $\zeta_r=0.01$, Fig. 3 shows the power generated for a range of values of C_p and θ_r. It is clear that the electromechanical coupling, θ_r has an optimum value, and that the piezoelectric capacitance, C_p, should be minimised. For rectangular transducers, these two requirements are often conflicting, and hence a shaped transducer may be able to help. Increasing the thickness of the piezoelectric material is another way to reduce the capacitance, but this may not be possible.

If a mode has a vibration node, then it is important that the transducer only covers parts of the beam where the curvature has the same sign (or the transducer could be segmented).

Consider now the system with an inductor. Suppose that the natural frequency of the beam has been tuned to the excitation frequency, so that $\omega=\omega_r$, as above. Furthermore assume that the electrical circuit has been tuned so that it also resonates at the excitation frequency (neglecting the electrical resistance and the electromechanical coupling), so that $\omega=\omega_e$ where $\omega_e^2=1/(LC_p)$. The voltage generated is then

$$V_p = \frac{m_r\omega_r^2\theta_r B_{Mr}u_0}{c_r/R_l + \theta_r^2}. \tag{29}$$

The voltage estimate is not affected by the capacitance of the piezoelectric transducer, although the inductance has to be changed as the transducer shape changes to ensure the electrical resonance occurs at the excitation frequency. For a given electrical resistance there will a finite value of coupling coefficient that gives a maximum voltage (and hence power) output, given by $\theta_r^2=c_r/R_l$, and the voltage tends to zero for very low or very high coupling coefficients.

V. OPTIMISING THE SHAPE OF THE PIEZOCERAMIC

For a given system, and excitation amplitude and frequency, the power harvested may be estimated using Eqs. (10)–(12) and (27). The coefficients of these equations depend on the shape of the transducer, which is approximated using the shape functions. Thus the shape is specified using the vector $\mathbf{f}$ and hence the power obtained is a function of $\mathbf{f}$, or

$$P_{\text{out}} = P_{\text{out}}(\mathbf{f}). \tag{30}$$

Unfortunately the form of the equations mean that a closed form solution for the optimum vector $\mathbf{f}$ cannot be obtained and the optimization problem must be solved numerically. However, this numerical optimization raises a number of issues. As the numerical approximation to the transducer shape is improved by using more finite elements, the number of variables to be optimised (i.e., the length of $\mathbf{f}$) increases leading to poor conditioning and the presence of many local optima. The problem of local optima is compounded by constraints on the width of the transducer, which cannot extend outside the width of the beam; often the global optimum is located on one of these constraint boundaries. The conditioning of the problem can be improved by also minimising the curvature of the piezoelectric material width,[20] given by

$$J_c = \mathbf{f}^{\mathrm{T}}\mathbf{E}\mathbf{f}, \tag{31}$$

where $\mathbf{E}$ is the stiffness matrix of a uniform free-free beam with a flexural rigidity of unity. The problem then becomes a multi-objective optimization that can be solved to obtain a Pareto front that highlights the trade-off between maximising power and minimising curvature.

The difficulty in the optimization problem does suggest an alternative, where the transducer shape is decoupled from the approximation inherent in $\mathbf{f}$. The shape may be specified using a small number of variables, and for a given set of values of these variables the corresponding $\mathbf{f}$ may be obtained and the power estimated. In this way the number of variables used in the optimization is not related to the quality of the approximation (given by the number of finite elements used). Furthermore promising candidate shapes, such as a rectangular transducer of variable length, may be implemented and easily optimised.

VI. NUMERICAL EXAMPLE

This example is designed to demonstrate that different shaped sensors can influence significantly the power gener-

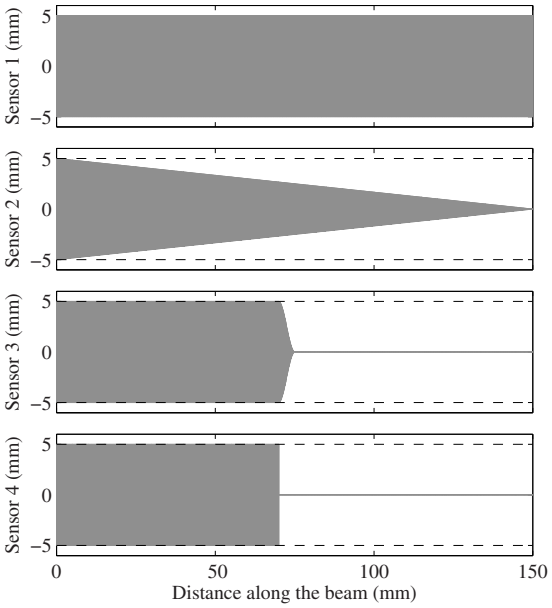

FIG. 4. (Color online) The shapes of the four candidate sensors. The dotted lines represent the extent of the steel beam.

ated by the harvester. Consider a steel beam of length 150 mm, breadth 10 mm, and thickness 3 mm, clamped at one end at a support that vibrates with an amplitude of 1 mm at a frequency of 110 Hz. Note that this is very close to the first natural frequency of the cantilever beam at 111.4 Hz. The damping ratio for the first mode is 1%. The piezoelectric material is 0.27 mm thick, with permittivity given by $\epsilon_{33}=1800\epsilon_0$, where the permittivity of free space is $\epsilon_0=8.854$ pF/m, and the piezoelectric constant is given by $e_{31}=-12.54$ C/m^2. The load resistance is 100 kΩ and no inductor is present. Four possible sensor shapes are tested, as shown in Fig. 4. The excitation frequency is very close to the first natural frequency and hence the harvester is resonant. Table I gives the capacitance, coupling coefficient and power output for the four sensors, and shows that the sensor shape has a significant effect on the power, through the competing influences of the capacitance and the coupling coefficient. Furthermore covering the whole beam with piezoelectric material generates about one third of the power of the case where the material only covers part of the beam. Table I gives the power estimated from the full model and also that estimated from the single mode model, showing that the latter is a good approximation. Note that the coupling coefficient is a single value based on the single mode approximation.

The difference between shapes 3 and 4 is the transition between the full width sensor and the no sensor. Sensor shape 4 is rectangular, whereas sensor shape 3 has a smooth transition over one finite element. Note that the rectangular transducer has slightly smaller area, and hence gives a smaller capacitance and coupling coefficient, but this results in a higher power output.

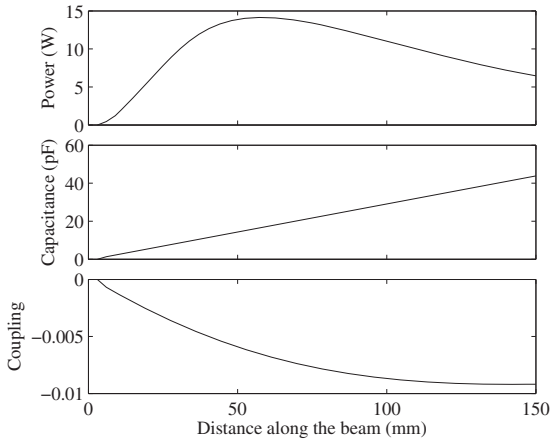

FIG. 5. The effect of varying the length of a rectangular transducer.

To demonstrate the effect the shape of the transducer can have, the length of sensor shape 3 is varied. All of the physical parameters remain unchanged, although the number of elements is now increased to 50. Figure 5 shows the effect of varying the transducer length (defined as the distance where the transducer remains at the full beam width) and shows that the capacitance increases with length, but the coupling coefficient decreases. This results in a length, just below 60 mm, that gives maximum power.

VII. CONCLUSIONS

The paper has developed the equations to estimate the power output from a beam energy harvester with a piezoelectric transducer. In particular the possibility of changing the shape of the transducer has been included by specifying the width and slope of the transducer at the finite element nodes. The transducer shape alters both the capacitance of the piezoelectric material, and also the coupling factor; often these parameters give rise to opposing effects on the power output. Four example shapes have been evaluated to determine the power output obtained, and this clearly shows that the shape has a significant influence. The example was a cantilever beam where the support was excited; other systems, for example, where a discrete mass is placed at the free end of the beam, may also be analyzed. A further example demon-

TABLE I. The properties and performance of the three shaped sensors.

Sensor number	Description	Capacitance (pF)	Coupling	Power output (W)	
				Full model	Single mode
1	Uniform	44.27	−0.00918	6.361	6.549
2	Triangular	22.14	−0.00667	10.17	10.76
3	Segment (smooth)	21.40	−0.00762	13.48	13.80
4	Segment (square)	20.66	−0.00748	13.65	13.98

strated that for a rectangular sensor there is a transducer length that gives the maximum power. The manner in which the governing equations are developed, where the transducer shape is determined by a small number of variables, gives the opportunity to optimise the sensor shape to maximise the power output. This is the subject of ongoing research.

[1]N. S. Hudak and G. G. Amatucci, J. Appl. Phys. **103**, 101301 (2008).
[2]H. A. Sodano, D. J. Inman, and G. Park, Shock Vib. Dig. **36**, 197 (2004).
[3]S. P. Beeby, M. J. Tudor, and N. M. White, Meas. Sci. Technol. **17**, R175 (2006).
[4]S. R. Anton and H. A. Sodano, Smart Mater. Struct. **16**, R1 (2007).
[5]S. Adhikari, M. I. Friswell, and D. J. Inman, Smart Mater. Struct. **18**, 115005 (2009).
[6]G. Litak, M. I. Friswell, and S. Adhikari, Appl. Phys. Lett. **96**, 214103 (2010).
[7]N. G. Stephen, J. Sound Vib. **293**, 409 (2006).
[8]J. M. Renno, M. F. Daqaq, and D. J. Inman, J. Sound Vib. **320**, 386 (2009).
[9]L. Mateu and F. Moll, J. Intell. Mater. Syst. Struct. **16**, 835 (2005).
[10]N. E. duToit and B. L. Wardle, AIAA J. **45**, 1126 (2007).
[11]A. Erturk and D. J. Inman, Smart Mater. Struct. **17**, 065016 (2008).
[12]A. Erturk and D. J. Inman, J. Vibr. Acoust. **130**, 041002 (2008).
[13]A. Erturk and D. J. Inman, J. Intell. Mater. Syst. Struct. **19**, 1311 (2008).
[14]A. Erturk and D. J. Inman, Smart Mater. Struct. **18**, 025009 (2009).
[15]F. Goldschmidtboeing and P. Woias, J. Micromech. Microeng. **18**, 104013 (2008).
[16]J. M. Dietl and E. Garcia, J. Intell. Mater. Syst. Struct. **21**, 633 (2010).
[17]J. Schoeftner and H. Irschik, Smart Mater. Struct. **18**, 125008 (2009).
[18]W. Kaal, S. Herold, and M. Kurch, Proceedings of IV ECCOMAS Thematic Conference on Smart Structures and Materials, *Porto, Portugal*, July 2009.
[19]C. J. Rupp, A. Evgrafov, K. Maute, and M. L. Dunn, J. Intell. Mater. Syst. Struct. **20**, 1923 (2009).
[20]M. I. Friswell, J. Sound Vib. **241**, 361 (2001).
[21]M. I. Friswell and S. Adhikari, Mech. Syst. Signal Process. **24**, 623 (2010).